Tellus (1997), 49B, 417–428
Printed in UK – all rights reserved

TELLUS
ISSN 0280–6509

Aerosol characteristics over coastal regions of the Arabian Sea

By S. K. SATHEESH and K. KRISHNA MOORTHY*, *Space Physics Laboratory, Vikram Sarabhai Space Centre, Trivandrum — 695 022, India*

(Manuscript received 28 January 1997; in final form 5 May 1997)

ABSTRACT

From aerosol spectral optical depths ($\tau_{p\lambda}$) at 10 wavelengths in the range 380 to 1025 nm estimated at different locations in the near and far coastal regions of the Arabian sea adjoining the western coast of central India, the spatial and spectral characteristics of coastal aerosols and the effect of the proximity to the (urban) continent are investigated. The Ångström parameters are deduced from $\tau_{p\lambda}$ values. A significant increase, both in aerosol optical depths at shorter (visible) wavelengths ($\lambda \leqslant 600$ nm) and the Ångström wavelength exponent are observed in the near coastal regions, suggesting an increase in the (relative) concentration of sub micron particles, apparently of anthropogenic origin. The Ångström turbidity coefficient remains nearly steady spatially, indicating a (spatially) uniform loading of large particles.

1. Introduction

Marine aerosols are primarily sea-salt particles or sea water droplets produced at the sea surface (Blanchard and Woodcock, 1980). About 30–35% of total (Global) aerosols produced are contributed by the oceans (Peterson and Junge, 1971; Prospero et al., 1983). Sub-micron aerosols in the marine boundary layer are believed to form condensation nuclei in the marine stratocumulus clouds and cause increase in cloud albedo (Charlson et al., 1987). They also modify the cloud droplet size distribution and change the cloud albedo (Fitzgerald, 1991) and thus strongly influence the radiative coupling between ocean and atmosphere (Charlson and Heintzenberg, 1995). Continental aerosols (natural and anthropogenic) are transported by winds to the oceanic environments and cause changes in the aerosol characteristics, particularly over oceanic regions adjoining urbanised and industrialised coastal land mass (Junge, 1972; Prospero, 1979; Hoppel et al., 1990). The sub micron aerosols from the industrial exhausts can act as condensation nuclei for the formation of cloud droplets which alters the albedo and cloud cover over adjacent oceanic regions with consequent effects on radiation, visibility and cloud characteristics of Marine Boundary Layer (MBL). Estimation of aerosol spectral optical depths over oceanic regions and studies on their spatial and temporal variations and dependence on various meteorological parameters are also important in ocean remote sensing. In this paper, we present the results of a study of the spatial and spectral characteristics of aerosol optical depths estimated at different regions in the near and far coastal locations of the Arabian sea, adjoining the western coast of central India, during March-April, 1996. The effects of the proximity of the urban and industrialised coastal land mass on the aerosol characteristics are examined.

2. Experimental details and data

Estimates of aerosol spectral optical depths have been made using a 10-channel multi-wavelength

* Corresponding author.

solar radiometer (MWR), at narrow wavelength bands centred at 380, 400, 450, 500, 600, 650, 750, 850, 935 and 1025 nm (selected using narrow band interference filters having full width half maximum band widths in the range 6 to 10 nm). Details of the instrument, designed following the principle of filter wheel radiometers (Shaw et al., 1973), are given elsewhere (Satheesh and Moorthy, 1996) and are not repeated here. The system had an overall field-of-view of $\approx 2°$. For such small values of the instrument field of view the error caused by the diffuse forward scattered radiation (from solar aureole) is negligibly small amounting to less than 1% at mid-visible for moderately turbid atmospheric conditions (with aerosol optical depths, $\tau_p \sim 0.5$) and still smaller at longer wavelengths (Shaw, 1976; Russell et al., 1993). As the aerosol optical depth encountered in this study has been generally less than 0.5 even at 380 nm and much smaller at longer wavelengths the error in τ_p due to the 2° field-of-view of the MWR is considered insignificant.

During the experiment the MWR has been taken onboard two scientific cruises of the Oceanographic Research Vessel (ORV) *Sagar Kanya* during its cruises #110 and #110A, dedicated mainly for oceanographic studies and collection of sea truth data for validation of the MOS (Modular Optoelectronic Scanner) payload onboard the Indian Remote sensing Satellite, IRS P-3. The 1st cruise (#110) was carried out during 29 February to 10 March, 1996 (prior to the launch of the satellite) while the second cruise (#110A) was during 13 to 20 April, 1996 (after the satellite has become operational). The respective cruise trajectories are shown in Fig. 1 with the daily position of the ship marked on it by filled circles. The numbers written on the cruise trajectory represents the date of observation. The programme was planned such that two sets of MWR observations would be possible on each day, one in the forenoon (FN) and the other in the afternoon (AN) period (if the sky was clear and cloud free). During the MWR observations, the ship was kept stationary at the location and each set of observation was of 2 to 3 h duration. From the MWR measurements, the columnar spectral optical depths, τ_λ, have been estimated following the Langley plot method and then subtracting the contributions due to molecular scattering and absorption from τ_λ, the details of which are given elsewhere (Moorthy et al., 1989; Moorthy et al., 1996), the aerosol spectral optical depths, $\tau_{p\lambda}$, are deduced. Molecular absorption by NO_2 is considered for the range 380 to 450 nm, by O_3 for 450 to 650 nm, and by water vapour at 850 nm. The contribution due to NO_2 absorption is typically ~ 0.003 (Russell et al., 1993) and that due to O_3 ranged from 0.002 to 0.03 at different wavelengths and is evaluated from the wavelength dependent absorption cross sections and climatological value of total O_3 for tropics. Using the MWR measurements at 935 nm and 1025 nm, the columnar water vapour content is estimated using the generalised transmission function (Leckner, 1978) and this is used to estimate the absorption at 850 nm. A total number of 17 data sets (of $\tau_{p\lambda}$) have been thus obtained, of which 13 sets were obtained during 1 to 8 March, 1996 (cruise #110) and 4 sets during 14 to 16 April 1996 (cruise #110A). Each day had two sets of data (one in the FN and the other in the AN period), except that on 1, 5 and 8 March and 14 April when no data was obtained in the FN and on 16 April when no data was obtained in the AN, owing to cloudy conditions. These 17 sets of $\tau_{p\lambda}$ formed the basic data for the present study.

3. General meteorological conditions

The general synoptic meteorological conditions during the cruise period have been quite similar to those expected to prevail over the central Indian region during early spring. There have been no synoptic weather systems and the sky conditions have been generally clear and cloud free for most of the time during cruise #110. However, during the April cruise (#110A) frequent cloud patches have been encountered and only four sets of MWR observations could be made, as mentioned earlier when there were no clouds in the neighbourhood of the sun. The prevailing winds have been generally steady and from the north-east, in line with the expected synoptic pattern (Rao, 1976; Das, 1986). The daily meteorological conditions during the cruise periods are obtained from the regular measurements (at three hourly intervals) of the surface meteorological parameters such as the wind speed, wind direction, relative humidity (RH), ambient temperature (T) and sea surface

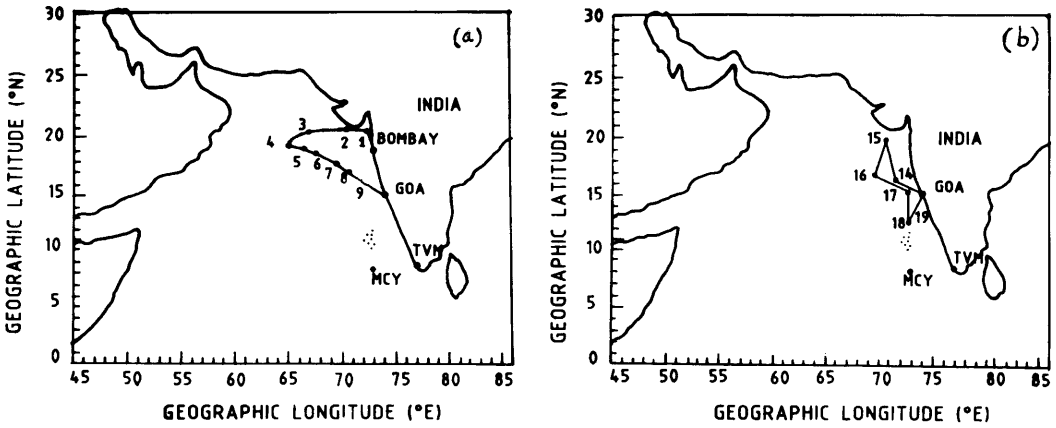

Fig. 1. Trajectory of the cruises; (a) for #110 and (b) for #110A.

temperature (SST), carried out onboard the ship. The measurements have been made at the deck level, ~10 m from the water level. The measured wind speed and direction have been corrected for the ship's velocity to determine the corresponding true values. Relative humidity and ambient temperature have been measured using wet and dry bulb thermometers while the SST has been obtained through measurements of bucket samples of sea water. The chronological variations of these parameters are shown in Fig. 2 for wind speed and direction and in Fig. 3 for SST, RH and T, respectively. The wind speed has been generally low with speeds in the range 2 to 6 m s^{-1} (Fig. 2a), maintaining a nearly steady northerly to north-easterly direction (Fig. 2b). The SST (Fig. 3a), showed an increasing trend from ~25°C to ~27°C in March and from ~28°C to 29°C during April cruises, showing the steady warming of the sea water as the sun approaches the equator and enters the northern hemisphere. Mean RH (Fig. 3b) showed a decrease from ~75% near Bombay coast to ~60% till 4 March 1996 and increased thereafter to a nearly steady value of ~80%. The mean ambient temperature (Fig. 3c) increased from ~26°C to 27°C during cruise #110 and from ~28°C to 30°C during cruise #110A. The slow and almost steady wind during the entire cruise period (Fig. 2) provided an opportunity to study the spatial variation of aerosol spectral optical depths over the coastal and interior Arabian sea and the effect of the proximity to continent on it, without any significant influence from wind enhanced local production of marine aerosols. Since the winds from the continental India passing over the Arabian sea being more or less steady and synoptic in nature, the ocean area close to the main land can be thought to be in a state of equilibrium (dynamical) with the continent as far as the aerosol distribution is concerned. In other words, the continental airmass might sustain an equilibrium aerosol concentration (subjected to loss by sedimentation and size transformation by coagulation and condensation only) such that there is no net rate of change of aerosol concentration at any given location; the offshore variation with distance being brought about by sedimentation, coagulation and condensation. Analysing the data with this perspective it is possible to use the aerosol optical depths, estimated for various parts of the coastal and interior oceanic regions on different days during the present investigation, to form a spatial mosaic of aerosol optical depths over the coastal Arabian sea.

4. Results and discussion

4.1. *Spatial variation of* $\tau_{p\lambda}$

The temporal variations of $\tau_{p\lambda}$ at all the MWR wavelengths are shown in Fig. 4, combined for both the cruises. In this representation, it is assumed that the aerosol characteristics remain more or less unchanged (over the oceanic regions

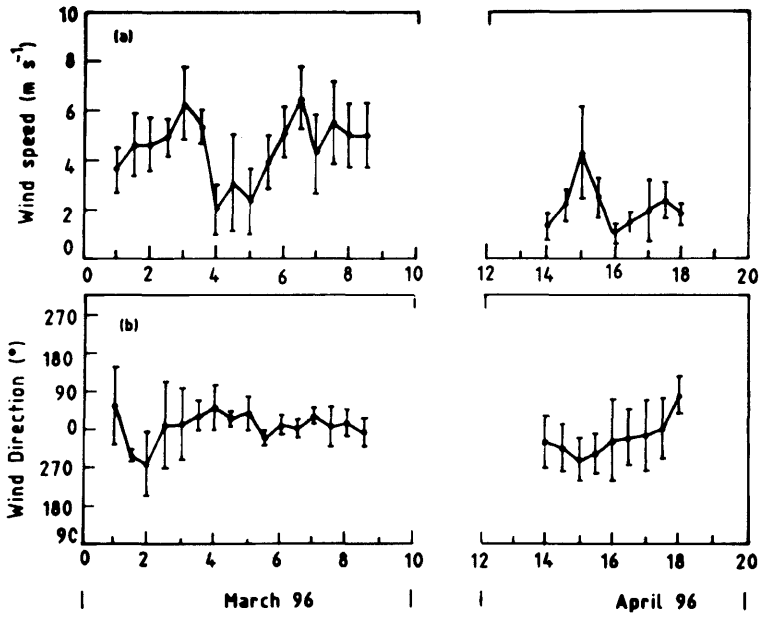

Fig. 2. Variation of mean surface wind speed (top) and direction (bottom). The vertical bars represent the standard deviation.

concerned) during the entire cruise period. The vertical bars through the points represent the estimated errors in τ_p which is the propagated sum of errors arising from uncertainties in the estimates of molecular scattering and absorption by NO_2, O_3 and H_2O; due to diffuse sky radiation entering the finite field of view of the MWR; and variations in the Langley intercept and the statistical errors arising in the Langley fit. The details of estimation of various errors are available in the literature (e.g., Shaw, 1976; Russell et al., 1993) and are not repeated. An analysis following the above shows that typical errors (excluding those from the least square fit) in the estimate of τ_p varied between 0.01 to 0.015 at different wavelengths and on different days. To this are added the propogated errors arising from the statistical errors of the least square (Langley) fit and the resultant is shown as error bars in Fig. 4. It can be seen from Fig. 1a that during 1 to 3 March, the ship track was very close to the coastal areas of the continental India (within $\sim$50 km). Subsequently, the ship moved in a south-west direction to the interior areas of the sea, reaching the farthest point on 4 March and returned along a south-east trajectory to reach Goa (marked in Fig. 1). During the period 4 to 8 March, the ship remained in the coastal regions much farther from the land. During the second cruise (Fig. 1b), the ship was almost in the coastal regions throughout except perhaps on 16 April 1996. In other words, during 1 to 3 March and 14 and 15 April, the observations are made closer to the main land compared to the other days when the MWR observations are made at more interior areas of the sea. In Fig. 5, the $\tau_{p\lambda}$ data are shown as a function of the distance, D, from the main land, calculated from Fig. 1, along the mean wind direction. In Fig. 5, the data obtained during cruise #110A are indicated by cross marks (x) separated from those obtained during cruise #110, which are represented by filled circles. It may be noted that the points from cruise #110A are well miscible with those of cruise #110 in as much as the combined data appears to form a single population, there by justifying the earlier assumption that the basic aerosol characteristics remained more or less the same during the March – April period. It can also be noticed (from Fig. 5) that there is, in general, a decrease in $\tau_{p\lambda}$ with increase in D. This decrease is more significant at shorter wavelengths ($\lambda \leqslant 600$ nm) and becomes increas-

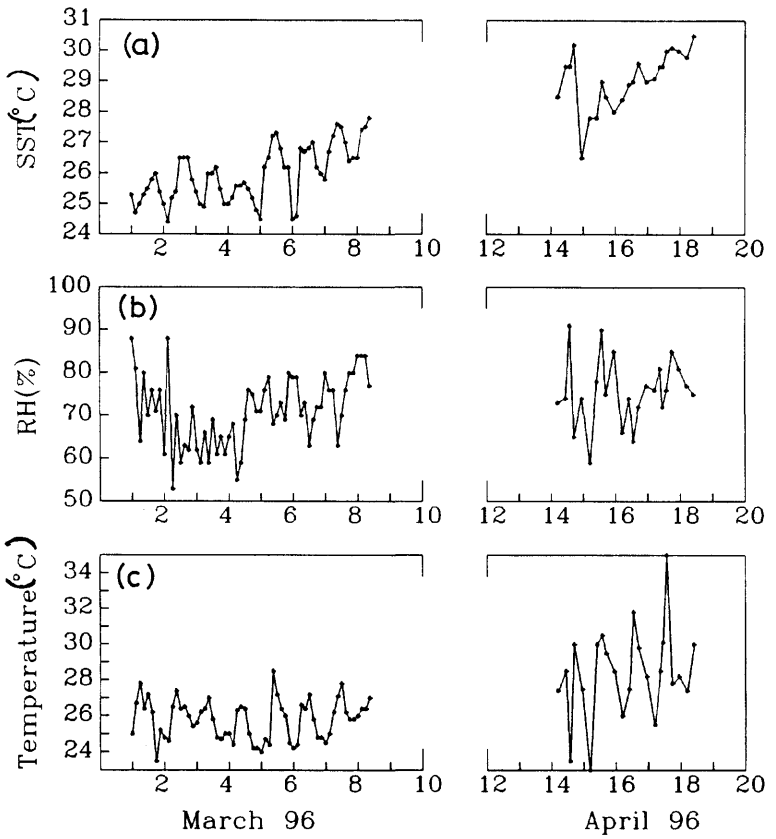

Fig. 3. Variations of SST (top), RH (middle) and T (bottom) during the cruise.

ingly dominant as λ decreases. At the longer (near IR) wavelengths the decrease is not easily discernible.

This aspect is examined further by obtaining the frequency of occurrence of $\tau_{p\lambda}$ separately for observations made at "near coastal" locations (which are more influenced by the proximity to the main land) and those made at "far coastal" locations. For this purpose, the MWR observations made at marine locations within ~ 150 km of the coast are considered to be near coastal and those made at $D > 200$ km as far coastal. For a typical wind speed of 2.5 m s^{-1}, the continental aerosols in the far coastal regions would be older than the nascent continental aerosols by about a day and would have undergone considerable size transformation (by coagulation and condensation processes) in the accumulation size range (Junge, 1963; Pruppacher and Klett, 1978; Hoppel et al., 1990). From Fig. 5 it can be seen that the near coastal case consists of eight sets and the far coastal case comprises of nine sets, of MWR observations. The frequency distributions of $\tau_{p\lambda}$ are shown in Fig. 6 (as histograms) separately for the near (shaded) and far coastal cases. It can be seen that for wavelengths below 600 nm, the values of $\tau_{p\lambda}$ for the near coastal regions are higher than those of the far coastal regions. As the wavelength increases, the two distributions overlap more and more and for $\lambda \geqslant 600$ nm, the distributions hardly differ. This feature is more clearly noticeable in Fig. 7, where the mean $\tau_{p\lambda}$ values for the near coastal (full line) and far coastal (dotted line) observations are plotted as a function of wavelength with the vertical bar representing the standard deviations. The difference between the mean values of $\tau_{p\lambda}$ becomes increasingly significant at shorter wavelengths.

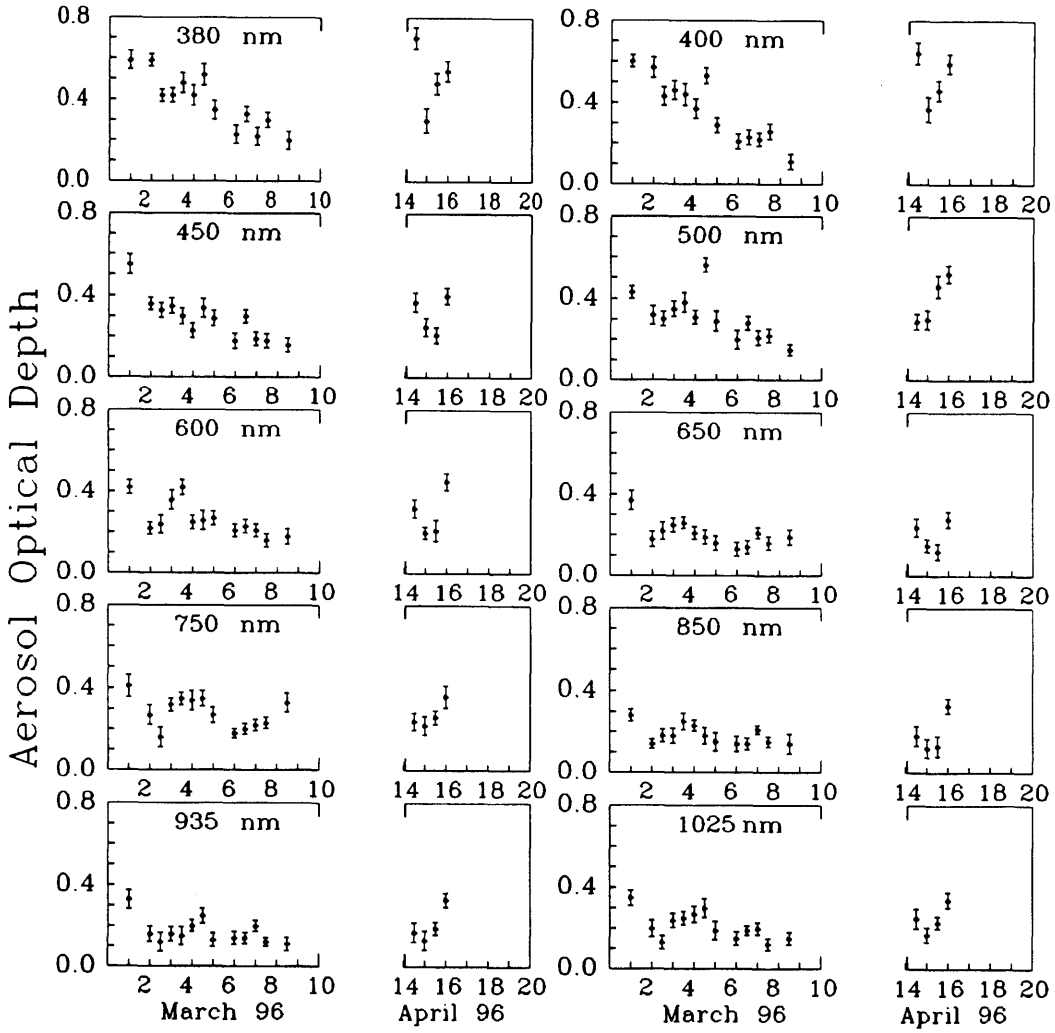

Fig. 4. Temporal variation of aerosol optical depths during the cruises. The vertical bars are the estimated errors in τ_p.

4.2. *Spectral characteristics of* $\tau_{p\lambda}$

The spectral characteristics of $\tau_{p\lambda}$ are indicative of the size distributions of the aerosols and the Ångström formula (Ångström, 1961; 1964), characterising the wavelength variation of $\tau_{p\lambda}$, is useful to draw inferences on the size distribution of aerosols. According to this formula,

$$\tau_{p\lambda}=\beta\lambda^{-\alpha}, \tag{1}$$

where β is the Ångström turbidity coefficient, equal to τ_p at $\lambda=1$ μm and α is the wavelength exponent. Relation (1) generally holds good when the aerosol size distribution follows an inverse power-law dependence on particle radius (r), of the form,

$$n_c(r)=N_0 r^{-\nu} \tag{2}$$

where, $n_c(r)$ is the columnar size distribution of aerosols, (giving the number density of aerosols in a vertical column of unit cross section, over a small radius interval dr centred at r), ν is the power law index and N_0 is a parameter dependent on the total number of aerosols (Junge, 1963). Under such conditions it has been shown (Junge,

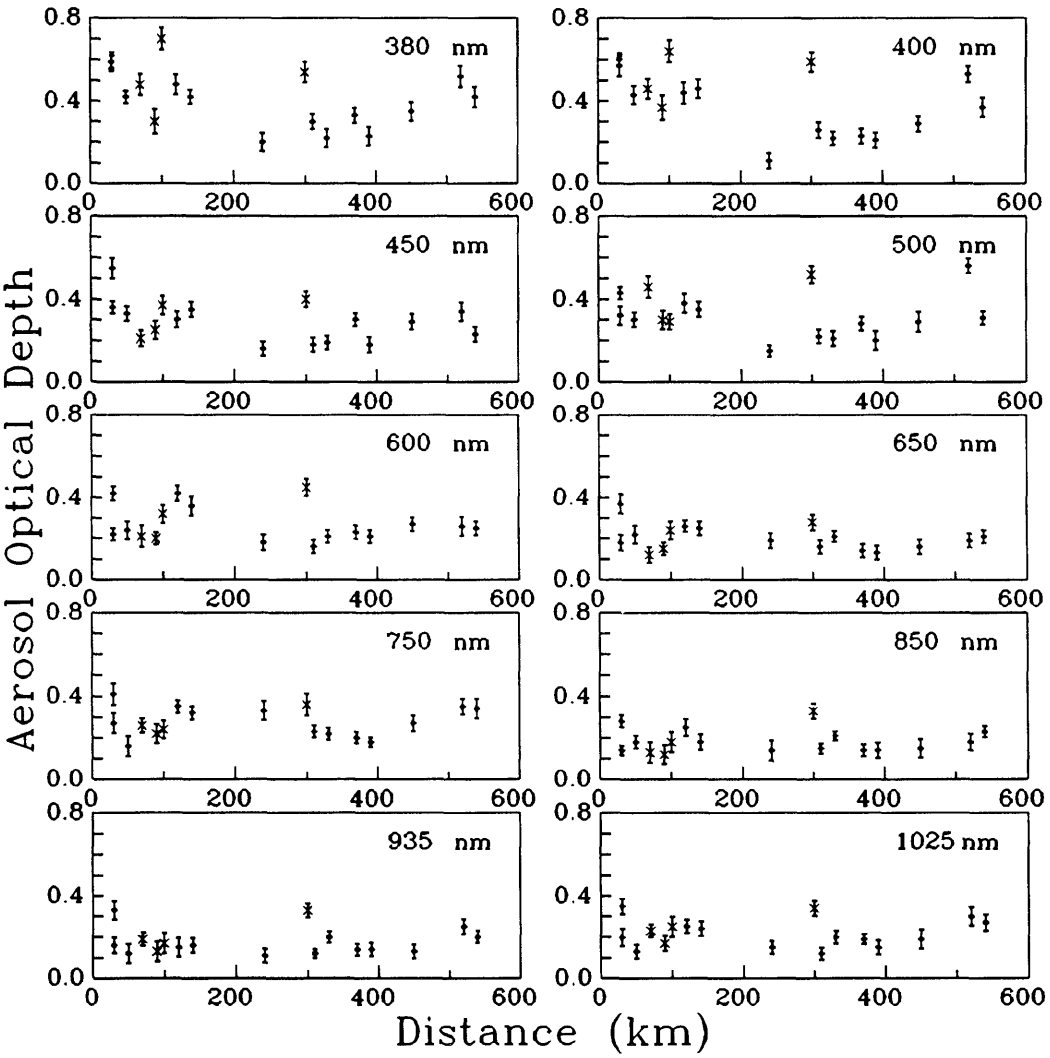

Fig. 5. Spatial variation of $\tau_{p\lambda}$ combined for both the cruises; the points from cruise #110A are identified by the cross symbols.

1952; Shaw et al., 1973; Tomasi et al., 1983) that,

$$\nu = \alpha + 3. \tag{3}$$

From this direct association between α and ν it follows that the lower values of α would mean smaller ν and the eq. (2) would depict a flatter particle size spectrum with $n_c(r)$ varying more slowly with r and thus supporting an increased dominance of larger particles in the size spectrum. On the other hand, for higher values of α (and hence ν) the particle size spectrum becomes steeper and $n_c(r)$ would have increased dominance of smaller particles. Thus if the spectral variation of $\tau_{p\lambda}$ can be described by eq. (1) and the exponent α is evaluated, it is possible to infer the broad features of the aerosol size distributions. Since the value of β (τ_p at $\lambda = 1$ μm) is a measure of the aerosol (column) loading (Tomasi et al., 1983) and depends more on large ($r > \sim 0.5$ μm) aerosol particles, its variation with D would be indicative of the spatial variation of large-particle concentration.

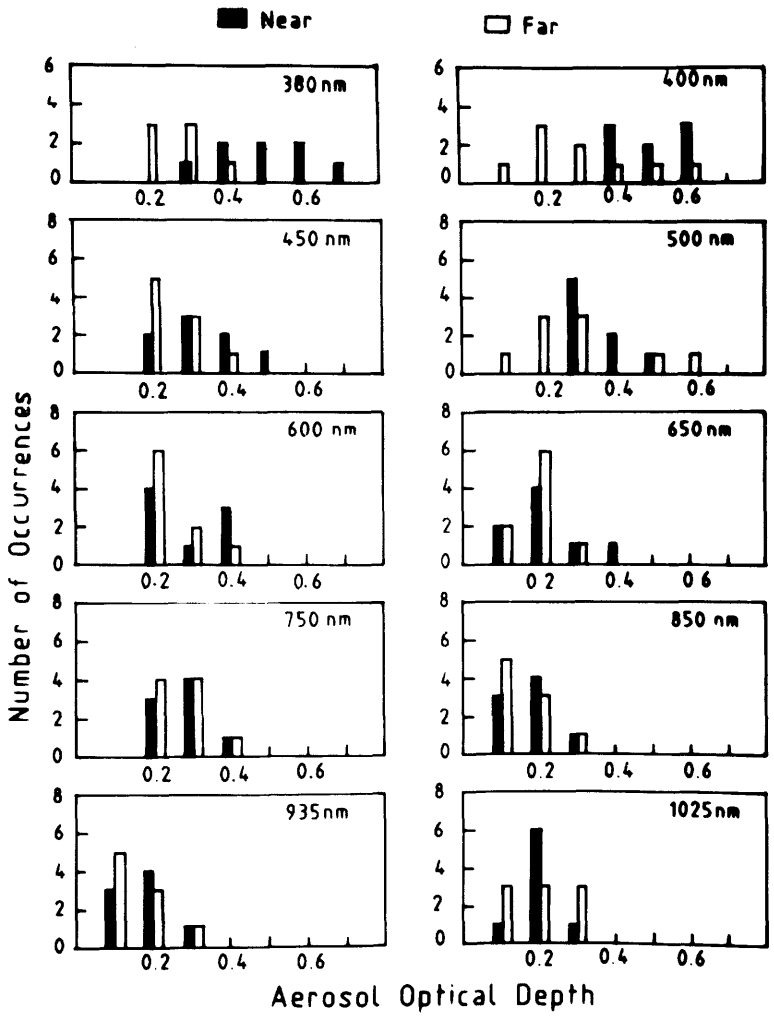

Fig. 6. Histograms showing the frequency distribution of $\tau_{p\lambda}$ separately for near coastal (shaded) and far coastal regions.

With this intention, $\tau_{p\lambda}$ values of individual sets of observations were examined for their agreement with eq. (1), by evolving a least square fit between $\tau_{p\lambda}$ and λ in a log-log scale. In general, a good agreement to eq. (1) has been obtained in all the cases with the correlation coefficient ρ lying in the range 0.60 to 0.98. Two representative examples are shown in Fig. 8 with the one having highest value of ρ (on the top) and the one having lowest value of ρ (on the bottom). The points are the experimentally observed values and the line is regression fitted to eq. (1). For the present case with 10 wavelengths, values of ρ exceeding 0.60 are significant at a significance level, $P=0.05$ or 95% (Fisher, 1970). The slope of the regression line gives the value of α while β is evaluated from the intercept. The mean variance of the regression slope (Kleinbaum and Kupper, 1978) is used to evaluate standard deviation of α. The variations of α and β are shown in Fig. 9 on a temporal scale and in Fig. 10 as a function of distance, D. The vertical bar on α represents the standard deviation.

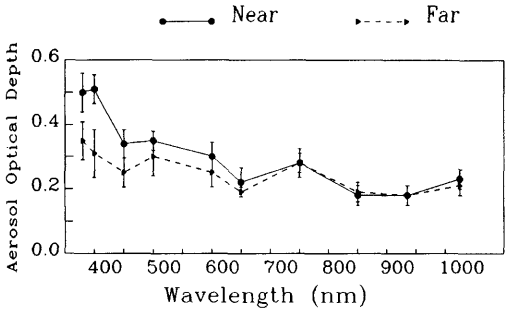

Fig. 7. Spectral variation of average aerosol optical depths for the near coastal (full line) and far coastal (dashed line) regions. Vertical bars are the standard deviations.

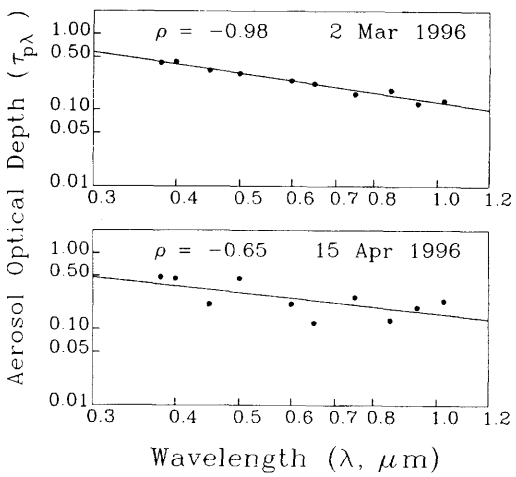

Fig. 8. Typical examples of wavelength variation of τ_p showing compliance with Ångström formula. The line is regression fitted to eq. (1).

It can be easily be seen from Fig. 10 that α decreases gradually as D increases. For the near coastal regions ($D < 150$ km), the values of α are, in general, significantly higher than those observed for the far coastal regions ($D > 200$ km). But it is quite interesting to note that β do not show any significant variation with distance, D, but remains nearly steady. The mean values of α and β, separately for these two coastal zones are given in Table 1.

As can be seen from Table 1, the mean value of α for the far coastal case is nearly half that of the near coastal case where as values of β do not show any appreciable change. As β (equal to τ_p at $\lambda = 1$ μm) is more sensitive to the larger aerosols ($r > \sim 0.5$ μm), the above observation indicates that the concentration of larger particles does not show significant spatial variations from close to the land to as far as ~ 550 km interior the sea. However, there is significant enhancement in the concentration of small particles in the near coastal regions (as can be inferred from the high values of α near coastal regions), which decreases sharply as one moves away from the coast.

Table 1. *Values of* α *and* β *for different coastal regions*

Coastal region	$\alpha \pm \sigma$	$\beta \pm \sigma$
near	0.97 ± 0.23	0.18 ± 0.06
far	0.50 ± 0.30	0.19 ± 0.06

The above features are attributed to a significant increase in the relative dominance of smaller particles (~ 0.01 to 0.3 μm) closer to the coast, because such particles have higher scattering and extinction efficiency at the shorter (visible) wavelengths compared to longer (near IR) wavelengths. The coastal regions of western central India is among the highly industrialised and urbanised regions in India. A number of oil refineries, thermal power stations and textile mills are situated in this region. Besides, Bombay (marked in Fig. 1) is among the largest urban centres in India with densest transport systems including automobiles, railways, aircrafts and ships. Thus it is highly probable that the gas-to-particle reaction products of the exhausts from these industrial and urban areas would dominate the coastal areas of north-western Arabian sea (areas under the present investigation). Under high levels of humidity in the coastal regions, these aerosols would undergo both physical and chemical changes. The processes such as condensation growth and coagulation could lead to an accumulation mode (Junge, 1963; Hoppel et al., 1990; 1994), the influence of this would manifest as an increase in τ_p at shorter wavelengths over marine areas adjacent to the coast. Continuous industrial activity would maintain a steady level of these sub micron aerosols over the continent which are then transported over to the marine areas by the north easterly offshore winds. The concentration of these

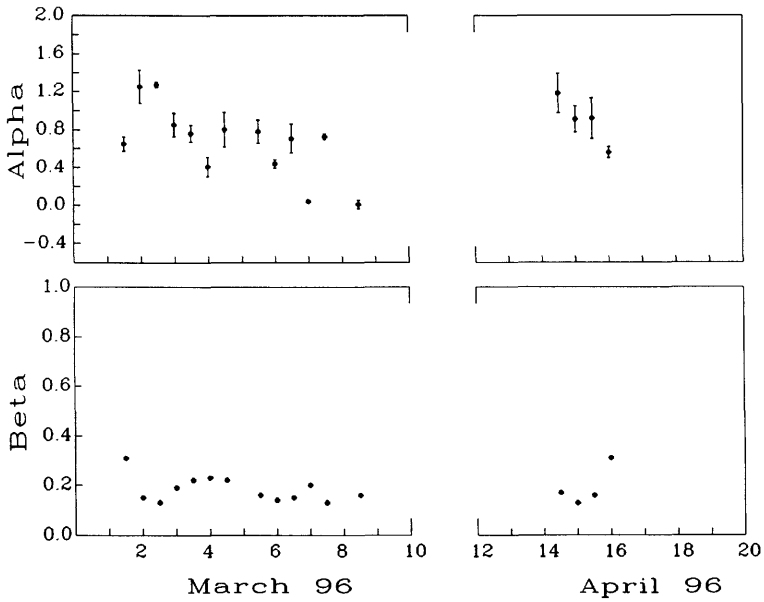

Fig. 9. Temporal variation of Ångström parameters.

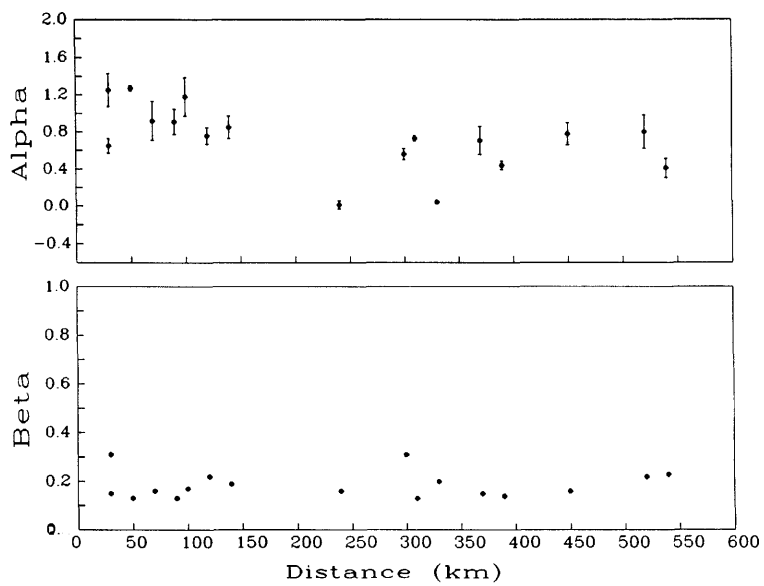

Fig. 10. Spatial variation of Ångström parameters.

(anthropogenic) sub micron particles would decrease rapidly as the distance from the coast increases (due to the above mentioned processes) which manifests as a rapid decrease in τ_p at shorter wavelengths as D increases. From extensive ship borne measurements Hoppel et al. (1989) have reported that as an air mass moves offshore from the continent, in the absence of clouds or precipitation, there is a rapid decay of submicron aerosol concentration as one moves farther off shore,

attributed mainly to the microphysical processes (condensation and coagulation). This leads to the appearance of an accumulation mode occurring at ~0.08 μm to 0.1 μm range (Hoppel et al., 1990; Fitzgerald, 1991). However, in the far coastal regions, the marine characteristics would assume importance. The low value of α for far coastal regions indicates that τ_p does not vary much with λ suggesting a flatter size distribution of aerosols, which is typical for maritime environment (Exton et al., 1985). The concentration of these particles appear to remain nearly steady spatially and temporally over the coastal regions as indicated by the nearly steady value of β. Surface measurements of aerosol mass concentration using a 10-stage Quartz Crystal Microbalance (QCM) impactor (covering a size range, 0.05 to 25 μm) over the coastal regions considered here, have also indicated an enhanced small particle concentration near the coast and a rapid decrease of these particles in the interior ocean region (A. Jayaraman, private communication). From pyrheliometer and sun photometer measurements at coastal regions of Bombay (Fig. 1), Mani et al. (1969) and Shirvaikar et al. (1976) have reported mean values of 1.0 for α and β to lie in the range 0.15 to 0.20. These values are very close to the values obtained for the near coastal regions in our study.

5. Conclusions

Our study of the characteristics of aerosols over coastal Arabian sea using spectral extinction measurements have revealed the following:

(1) There is a significant enhancement of aerosol optical depth at shorter wavelengths ($\lambda \leqslant 600$ nm) in the near coastal regions compared to the far coastal regions.

(2) The wavelength variation of $\tau_{p\lambda}$ can be represented by the Ångström formula. The Ångström wavelength exponent (α) has a mean value of 0.5 for the far coastal regions indicating a flatter size spectrum of aerosols. In the near coastal regions the value of α nearly doubles, indicating a significant enhancement of small particles attributed to be of industrial and urban origin, originating from the highly industrialised continental regions adjoining the sea.

6. Acknowledgements

This study formed part of the IRS P-3 validation experiment undertaken by ISRO. The authors are grateful to the Department of Ocean Development (DOD), Delhi and Director, National Institute of Oceanography (NIO), Goa for providing the ship board facilities. We are also thankful to Dr B. V. Krishna Murthy, Director, Space Physics Laboratory for the useful discussions.

REFERENCES

Ångström, A. 1961. Techniques of determining the turbidity of the atmosphere. *Tellus* **13**, 214–223.

Ångström, A. 1964. The parameters of atmospheric turbidity. *Tellus* **16**, 64–75.

Blanchard, D. C. and Woodcock A. H. 1980. The production, concentration and vertical distribution of the sea-salt aerosol. *Ann. of the N. Y. Academy of Sciences* **338**, 330–347.

Charlson, R. J., Lovelock, J. E., Andreae, M. O. and Warren, S. G. 1987. Oceanic phytoplankton, atmospheric sulfur, cloud albedo and climate. *Nature* **326**, 655–661.

Charlson, R. J. and Heintzenberg, J. 1995. *Aerosol forcing of climate* John Wiley & Sons, New York, 416pp.

Das, P. K. 1986. *Monsoons*, 5th IMO Lecture. WMO-No.613, World Meteorological Organization, Ganeva, Switzerland, pp. 29–55.

Exton, A. J., Latham J., Park P. M., Perry S. J. and Smith M. H. 1985. The production and dispersal of marine aerosol. *Q. J. Roy. Meteorol. Soc.* **111**, 817–837.

Fisher, R. A. 1970. *Statistical methods for research works.* Oliver & Boyd, Edinburgh.

Fitzgerald, J. W. 1991. Marine Aerosols-A review. *Atmos. Environ.* **25(A)**, 533–545.

Hoppel, W. A., Fitzgerald, J. W., Frick, G. M., Larson, R. E. and Mack, E. J. 1989. *Atmospheric aerosol size distributions and optical properties found in the Marine boundary layer over the Atlantic Ocean.* NRL Report 9188, Washington DC, USA, pp 1–75.

Hoppel, W. A., Fitzgerald, J. W., Frick G. M. and Larsen, R. E. 1990. Aerosol size distributions and optical properties found in the marine boundary layer over the Atlantic ocean. *J. Geophys. Res.* **95** 3659–3686.

Hoppel. W. A., Frick, G. M., Fitzgerald, J. W. and Larson, R. E. 1994. Marine boundary layer measurements of a new particle formation and the effects of non-precipitating clouds have on aerosol size distribution. *J. Geophys. Res.* **99**, 14,443–14,459.

Junge, C. E. 1952. *Gesetzmäßigkeiten in der Größenverteilumg atmosphärischer Aerosol über dem Kontinent.*

Report 35 Deutscher Wetterdienst in der US-Zone, pp 261–277.

Junge, C. E. 1963. *Air chemistry and Radioactivity.* Academic Press Inc., New York, USA, pp 111–208.

Junge, C. E. 1972. Our knowledge of the physicochemistry of aerosols in the undisturbed marine environments. *J. Geophys. Res.* **77**, 5183–5200.

Kleinbaum, D.G and Kupper, L. L. 1978. *Applied regression analysis and other multi-variable methods.* Duxburg, Boston, 49 pp.

Leckner, B. 1978. The spectral distribution of solar radiation at the earth's surface-elements of a model. *Sol. Energy* **20**, 143–150.

Mani, A., Chacko, O. and Hariharan, S. 1969. A study of Ångström's turbidity parameters from solar radiation measurements in India. *Tellus* **21**, 829–843.

Moorthy, K. K., Nair, P. R. and Krishna Murthy, B. V. 1989. Multiwavelength solar radio meter network and features of aerosol spectral optical depth at Trivandrum. *Ind. J. Radio Space Phys.* **18**, 194–201.

Moorthy, K. K., Nair, P. R., Krishna Murthy B. V. and Satheesh, S. K. 1996. Time evolution of the optical effects and aerosol characteristics of Mt.Pinatubo origin from ground based observations. *J. Atmos. Terr. Phys.* **58**, 1101–1116.

Peterson, J. T. and Junge, C. E. 1971. Sources of particulate matter in the atmosphere. In: *Man's impact on the climate*, ed. W. H. Mathews, W. W. Kellog and G. D. Robinson. MIT Press, Cambridge, Mass., pp 310–320.

Prospero, J. M. 1979. Mineral and sea-salt aerosol concentrations in various ocean regions. *J. Geophys. Res.* **84**, 725–731.

Prospero, J. M., Charlson, R. J., Mohnen, V., Jaenicke, R., Delany, A. C., Moyers, J. Zoller W. and Rahn, K. 1983. The atmospheric aerosol system. An overview. *Rev. of Geophys. and Space Phys.* **21**, 1607–1629.

Pruppacher, H. R. and Klett, J. D. 1978. *Microphysics of clouds and precipitation.* D. Reidel Publishing Co., Hingham, Masschusetts, USA, pp 364–371.

Rao, Y. P. 1976. *South West Monsoon.* Meteorol. Monograph Synoptic Meteorology, No.1/1976, IMD, New Delhi, India.

Russell, P. B., Livingston, J. M., Dutton, E. G., Pueschel, R. F., Reagon, J. A., Defoor, T. E., Box, M. A., Allen, D., Pilewskie, P., Herman, B. M., Kinnie, S. A. and Hofmann, D. J. 1993. Pinatubo and Pre-Pinatubo optical depth spectra: Mauna Loa measurements, comparisons, inferred particle size distribution, radiative effects and relationship to Lidar data. *J. Geophys. Res.* **98**, 22,969–22,985.

Satheesh, S. K. and Moorthy, K. K. 1996. Atmospheric total ozone content from spectral extinction measurements. *Ind. J. Radio Space Phys.* **25**, 204–210.

Shaw, G. E. 1976. Error analysis of multiwavelength sun photometry. *Pure. Appl. Geophys.* **114**, 1–14.

Shaw, G. E., Reagan, J. A. and Herman, B. M. 1973. Investigations of atmospheric extinction using direct solar radiation measurements made with a multiple wavelength radiometer. *J. Appl. Meteorol.* **12**, 374–380.

Shirvaikar, V. V., Sitaraman, V. and Sastry P. L. K. 1976. A study of the wavelength exponent of aerosol scattering using Volz sun photometer. *Tellus* **4**, 373–376.

Tomasi, C., Caroli, E. and Vitale, V. 1983. Study of the relationship between Ångström's wavelength exponent and Junge's particle size distribution exponent. *J. Climate and Appl. Meteorol.* **22**, 1707–1715.